

Electronic Supporting Information for Decorrelated Singlet and Triplet Exciton Delocalization in Acetylene-Bridged Zn-Porphyrin Dimers

Hasini Medagedara,[†] Mandefro Y. Teferi,[‡] Sachithra T. Wanasinghe,[†]
Wade Burson,[†] Shahad Kizi,[†] Bradly Zaslona,[†] Kristy Mardis,[¶] Jens
Niklas,[‡] Oleg G. Poluektov,^{*,‡} and Aaron S. Rury^{*,†}

[†]*Department of Chemistry, Wayne State University, Detroit, MI 48202, USA*

[‡]*Chemical Sciences and Engineering Division, Argonne National Laboratory, Lemont, IL 60439,
USA*

[¶]*Department of Chemistry, Physics, and Engineering Sciences, Chicago State University,
Chicago, IL, 60628, USA*

E-mail: oleg@anl.gov; arury@wayne.edu

List of Figures

S1	Structures of Fb-M , Fb ₂ U-D, and ZnFbU-D.	S3
S2	Proton NMR spectra of F ₃₀ Zn ₂ U-D in CDCl ₃	S4
S3	Proton NMR spectra of Zn ₂ U-D in CDCl ₃	S4
S4	MALDI-TOF mass spectra of F ₃₀ Zn ₂ U-D and Zn ₂ U-D	S5
S5	Comparisons between the measured Q state absorption (green) and fluorescence (red) spectra of Zn-M (top left panel), F ₂₀ Zn-M (top right panel), Zn ₂ U-D (bottom left panel), and F ₃₀ Zn ₂ U-D (bottom right panel).	S7
S6	Transient transmission spectra of Zn-M (top left panel), F ₂₀ Zn-M (top right panel), Zn ₂ U-D (bottom left panel), and F ₃₀ Zn ₂ U-D (bottom right panel) after photoexcitation at 2.85 eV.	S8
S7	Comparisons between the measured (solid green) and simulated (dashed red) spectra of Zn-M (top panel) and Zn ₂ U-D (bottom panel), which also show the assignments of transitions at the X ⁺ , X ⁻ , Y ⁺ , Y ⁻ , Z ⁺ , and Z ⁻ canonical field strengths.	S9

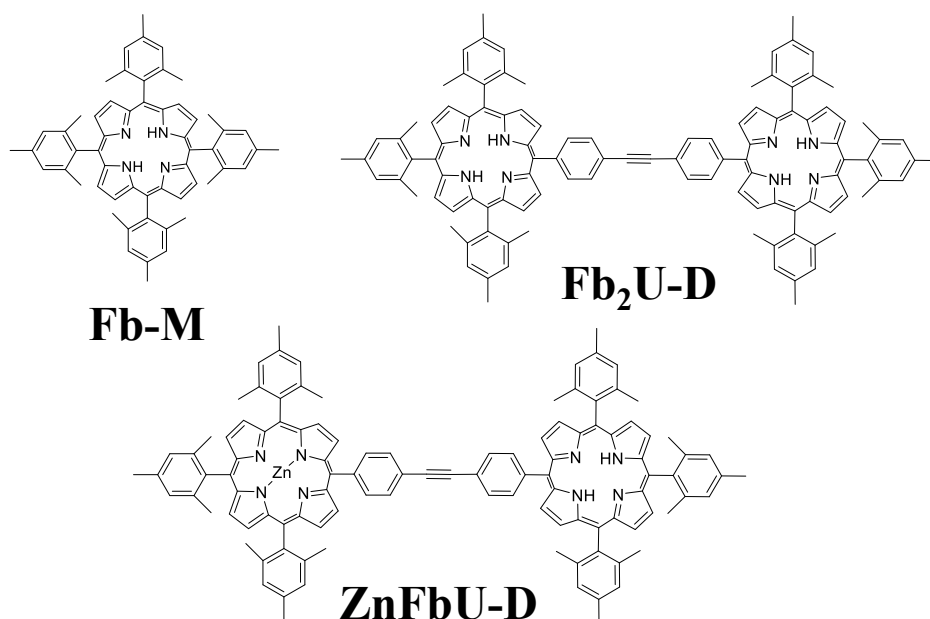


Figure S1: Structures of Fb-M , Fb₂U-D, and ZnFbU-D.

1 Chemical Structures of Model Chromophores

Fig. S1 shows the structures of Fb-M, Fb₂U-D, and ZnFbU-D, which were studied as models for time-resolved EPR and ENDOR measurements of these molecules' triplet states.

2 Synthesis and Characterization of Model Porphyrin Macromolecules

The chemical compounds mesitaldehyde, 4-iodophenyl benzaldehyde, 2,3-dichloro-5,6-dicyano-1,4-benzoquinone, triethylamine and pentafluoro benzaldehyde were purchased from Oakwood Chemical USA. Pyrrole, boron trifluoride etherate, 4-[2-(trimethylsilyl) ethynyl]benzaldehyde, tetrabutylammonium fluoride on silica, tris(dibenzylideneacetone)dipalladium(0), triphenylarsine, sodium bicarbonate and zinc acetate were purchased from Sigma Aldrich USA. Freebase porphyrin monomer 5,10,15,20-tetrakis(pentafluorophenyl)porphyrin was purchased from TCI Chemical USA. Bio-Beads SX-1 styrene divinylbenzene beads for size exclusion chromatography was

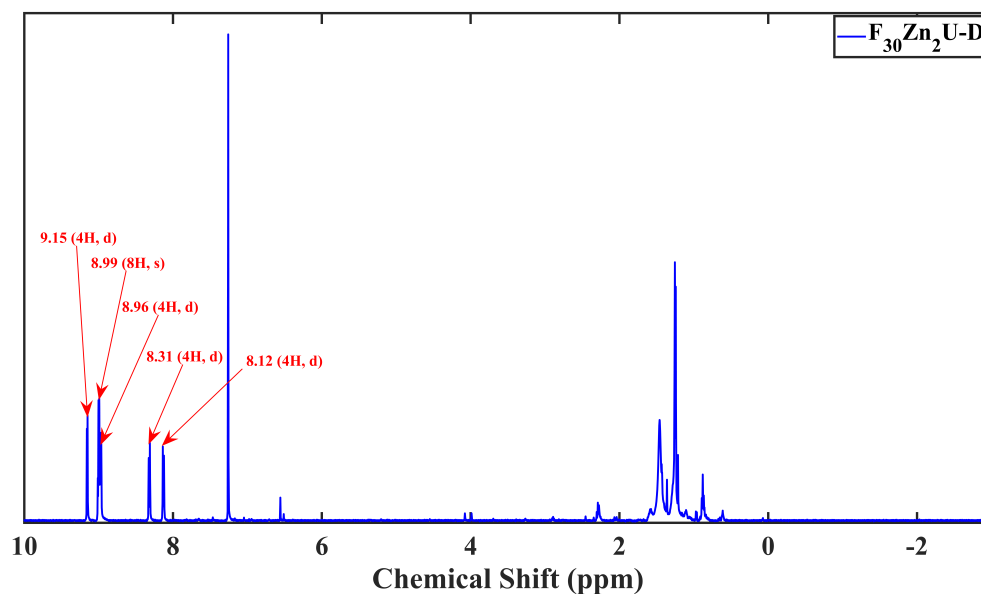


Figure S2: Proton NMR spectra of $F_{30}Zn_2U-D$ in $CDCl_3$

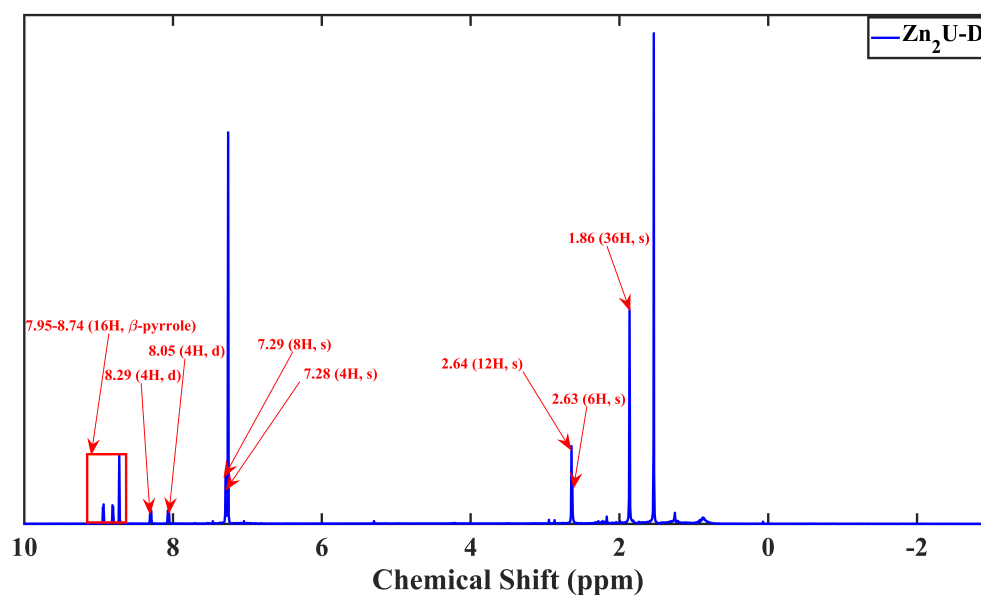


Figure S3: Proton NMR spectra of Zn_2U-D in $CDCl_3$

purchased from Bio-Rad Laboratories USA. Synthesis of 5,10,15,20-tetrakis(mesityl)porphyrin (Fb-M), zinc porphyrin monomers and dimers were carried out according to previously reported studies. The synthesized porphyrins were characterized using nuclear magnetic resonance (NMR) in $CDCl_3$ and MALDI-TOF mass spectrometry.

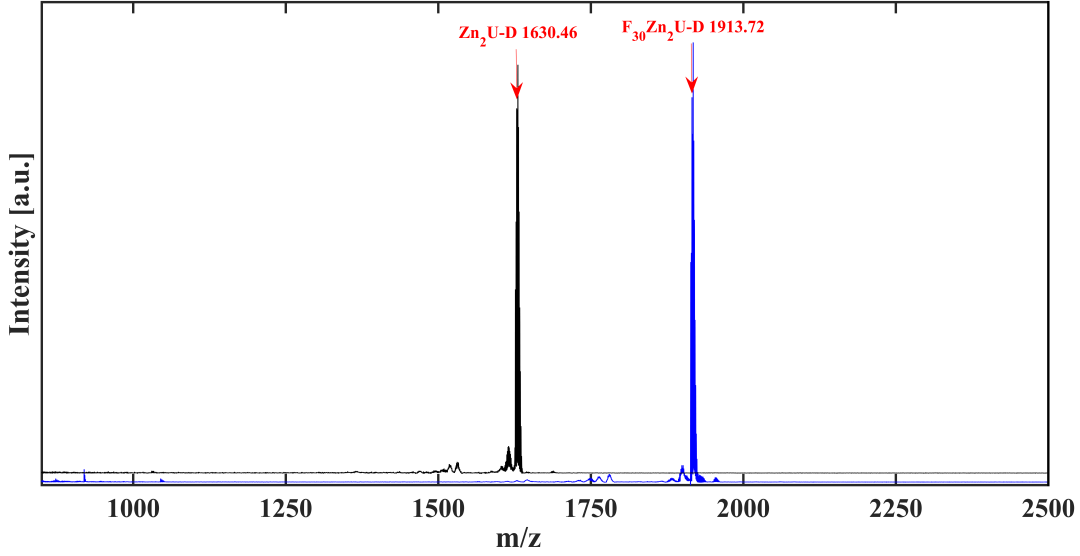


Figure S4: MALDI-TOF mass spectra of $F_{30}Zn_2U-D$ and Zn_2U-D

3 Steady-State UV-vis Absorption and Fluorescence Spectra

3.1 Soret Resonance

We modeled the absorption spectrum of Zn_2U-D using the following equation,

$$A(E) = I_1 \exp\left(-\left[\frac{E - E_1}{2\Delta E_1}\right]^2\right) + I_2 \exp\left(-\left[\frac{E - E_2}{2\Delta E_2}\right]^2\right) + I_3 \exp\left(-\left[\frac{E - E_3}{2\Delta E_3}\right]^2\right) + mE + b, \quad (S1)$$

where we assign the peaks corresponding to the first, second, and fourth terms of Eq. (S1) as resulting from the x-polarized 0-0, the y-polarized 0-0, and 0-1 vibronic transition. Given their low intensities, we propose the x- and y-polarized 0-1 vibronic transitions do not couple in Zn_2U-D . We assign the third term in Eq. (S1) as stemming from H-aggregates that form in face-to-face orientations in the solution at sufficiently high concentrations. The last terms of Eq. (S1), $(mE + b)$, represent a sloping background to the spectra.

We modeled the absorption spectrum of $Zn-M$, $F_{20}Zn-M$, and $F_{30}Zn_2U-D$ using the following

equation,

$$\begin{aligned}
 A(E) = & I_1 \exp\left(-\left[\frac{E - E_1}{2\Delta E_1}\right]^2\right) + I_2 \exp\left(-\left[\frac{E - E_2}{2\Delta E_2}\right]^2\right) \quad (\text{S2}) \\
 & + I_3 \exp\left(-\left[\frac{E - E_3}{2\Delta E_3}\right]^2\right) + mE + b,
 \end{aligned}$$

where we assign the peaks corresponding to the first and third terms of Eq. (S2) as resulting from the 0-0 and 0-1 vibronic structures of the Soret resonance of individual molecules of each porphyrin species. We propose the second term in Eq. (S1) stems from H-aggregates that form in face-to-face orientations in the solution at sufficiently high concentrations. The terms $(mE + b)$ represent a sloping background in each spectrum. We report the important model values found by fitting our data to Eqs. (S1) and in (S2) Table SI.

Table S1: Quantitative comparison between the intensities, energies, and widths of the Soret absorption peaks of Zn-M, F₂₀Zn-M, Zn₂U-D and F₃₀Zn₂U-D in toluene

Sample	I ₁ [O. D.]	E ₁ [eV]	ΔE ₁ [meV]	I ₂ [O. D.]	E ₂ [eV]	ΔE ₂ [meV]	I ₃ [O. D.]	E ₃ [eV]	ΔE ₃ [meV]
Zn-M	0.676±0.041	2.94±0.01	19.7±0.2	0.082±0.004	3.00±0.00	14.6±1.8	0.048±0.006	3.09±0.00	28.11±2.7
F ₂₀ Zn-M	0.402±0.001	2.94±0.00	23.2±0.1	0.043 ±0.005	3.01±0.00	17.5±0.5	0.041±0.001	3.08±0.00	39.5±2.7
Zn ₂ U-D	0.425±0.044	2.90±0.01	26.6±1.7	0.199±0.080	2.96±0.01	21.2±2.5	0.044±0.006	3.042±0.03	50.0± 15.1
F ₃₀ Zn ₂ U-D	0.376±0.010	2.92±0.00	30.7±0.9	-	-	-	0.040±0.004	3.04±0.02	58.8±12.6

3.2 Q Resonance

The panels of Fig. S2 show comparisons between the measured Q state absorption and fluorescence spectra of Zn-M, F₂₀Zn-M, Zn₂U-D, and F₃₀Zn₂U-D. By comparing the structure of the spectra corresponding to monomers and dimer (Zn-M to Zn₂U-D and F₂₀Zn-M to F₃₀Zn₂U-D) we find no qualitative evidence of intermolecular Q-state exciton delocalization in either dimer. From this lack of evidence we propose the Q-state excitons must remain localized in one of the two porphyrin sub-units of Zn₂U-D.

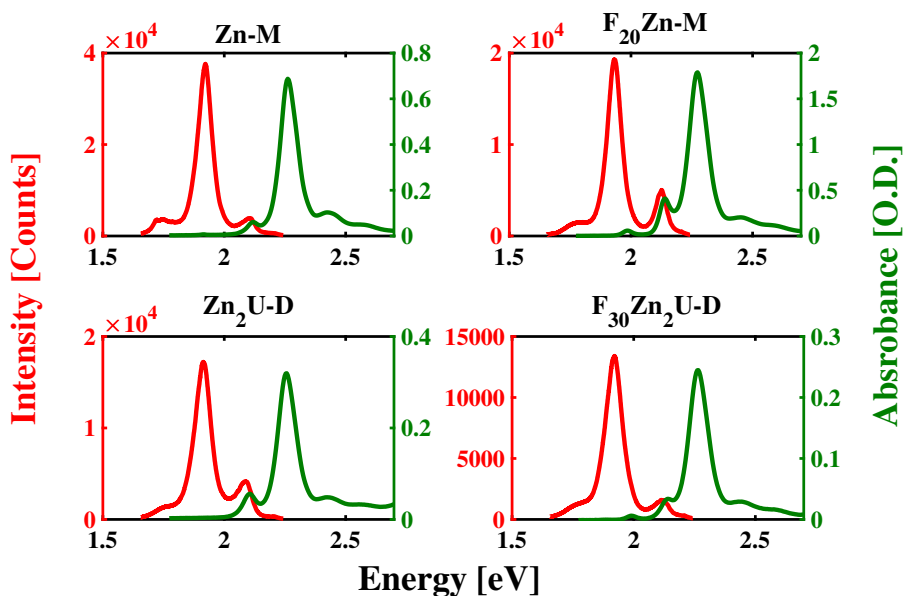


Figure S5: Comparisons between the measured Q state absorption (green) and fluorescence (red) spectra of Zn-M (top left panel), F_{20} Zn-M (top right panel), Zn_2 U-D (bottom left panel), and $F_{30}Zn_2$ U-D (bottom right panel).

4 Transient Transmission Spectra

The panels of Fig. S3 show the broadband transient transmission spectra of Zn-M, F_{20} Zn-M, Zn_2 U-D, and $F_{30}Zn_2$ U-D across the visible region of the excited state spectra following photoexcitation with a 2.85 eV (435 nm) pump pulse. The blue and red regions of the spectra indicate excited state absorption and ground state bleaching, respectively. The rise of stimulated emission appears as a feature at 1.9 eV due to depleted excited state absorption. Kinetic traces of these dynamics are shown in Fig. 3 of the main manuscript.

5 Time-Resolved EPR Spectra

The panels of Fig. S4 show comparisons between the measured and simulated TR-EPR spectra of Zn-M and Zn_2 U-D. These panels include assignments of triplet transitions at the X^+ and X^- canonical field strengths. These transitions overlap with those of the Z^+ and Z^- canonical fields and complicate our analysis of these molecule's triplet ENDOR spectra.

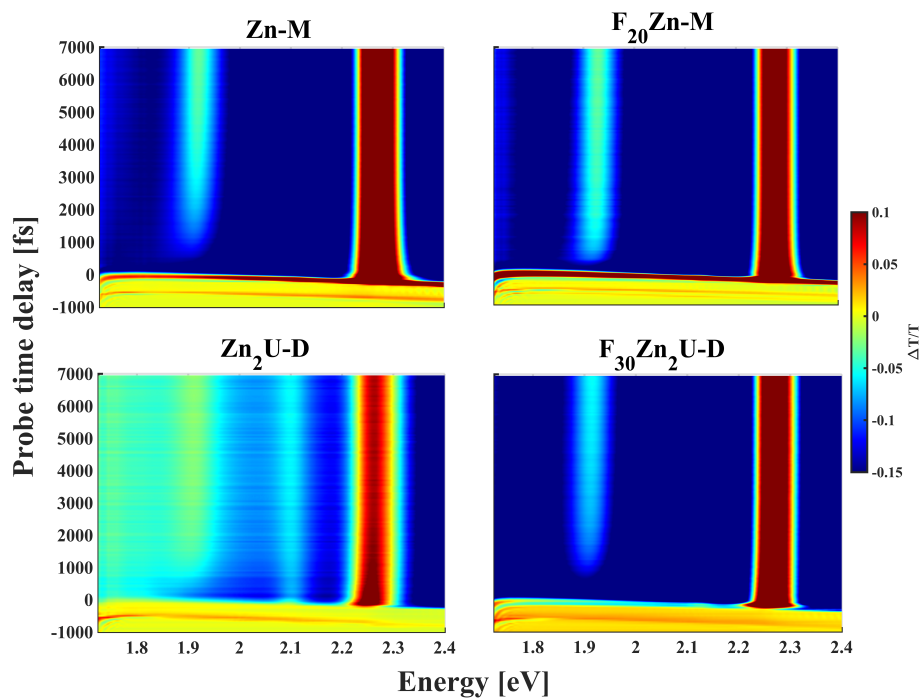


Figure S6: Transient transmission spectra of Zn-M (top left panel), F_{20} Zn-M (top right panel), Zn_2 U-D (bottom left panel), and F_{30} Zn_2 U-D (bottom right panel) after photoexcitation at 2.85 eV.

References

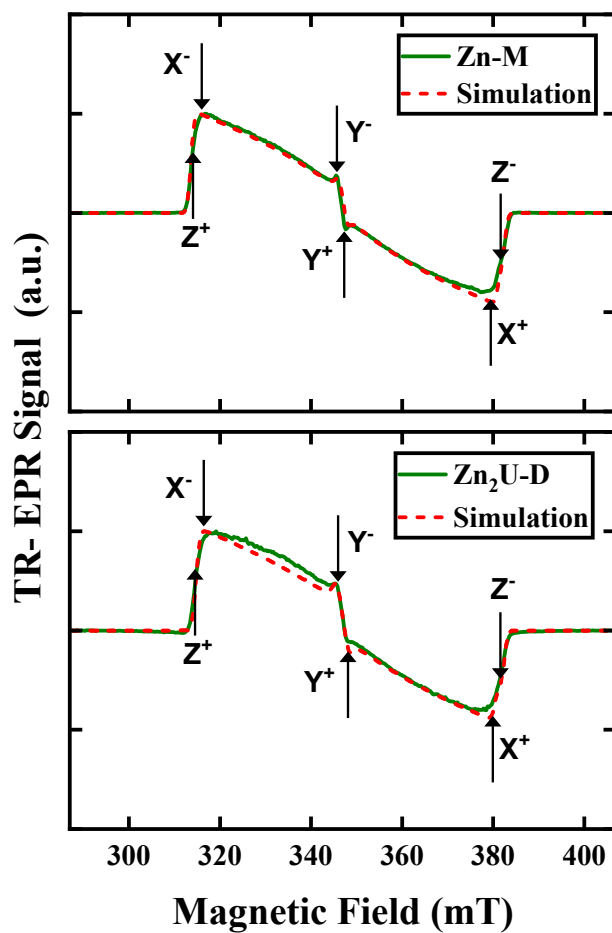


Figure S7: Comparisons between the measured (solid green) and simulated (dashed red) spectra of Zn-M (top panel) and Zn₂U-D (bottom panel), which also show the assignments of transitions at the X⁺, X⁻, Y⁺, Y⁻, Z⁺, and Z⁻ canonical field strengths.